Turkish Journal of Electrical Engineering & Computer Sciences

http://journals.tubitak.gov.tr/elektrik/

Research Article

Turk J Elec Eng & Comp Sci
(2017) 25: 2910 – 2921

doi:10.3906/elk-1605-40

A new approach for minimizing torque ripple in a BLDC motor drive with a front end IDO dc-dc converter

Ramya AMIRTHALINGAM*, Balaji MAHADEVAN
Department of Electrical Engineering, SSN College of Engineering, Tamil Nadu, India

Received: 04.05.2016 • **Accepted/Published Online:** 11.11.2016 • **Final Version:** 30.07.2017

Abstract: This paper proposes a front end integrated dual output (IDO) dc-dc converter for commutation torque ripple reduction in a permanent magnet brushless DC (BLDC) motor drive. The current ripple owed to the inductance and resistance of the motor during commutation instant results in torque ripple. In this work the dc link voltage of the converter is varied at commutation instants to minimize current ripple and hence torque ripple. The wider output range and faster response of the IDO converter make it a suitable choice as a front end converter for minimizing torque ripple. Simulation results validate the proposed converter for the BLDC motor drive. Experimental analysis of a conventional drive is performed to verify the simulation results.

Key words: Commutation torque ripple, brushless DC motor, integrated dual output dc-dc converter

1. Introduction

Permanent magnet BLDC motors are gaining recognition in the electric drive market due to their high efficiency, low maintenance, high power density, and low electromagnetic interference problem [1–5]. Commutation torque ripple is a serious drawback of the BLDC motor that occurs due to current distortions during phase transitions. Torque ripple in a BLDC motor drive gives rise to mechanical vibrations and acoustic noise. Researchers have proposed modified PWM control, DC bus voltage control, current control, torque control, and phase conduction control based torque ripple minimization strategies for BLDC motor drives.

In [6], the torque and torque ripple in a BLDC motor drive is analyzed in detail with the commutation effect taken into consideration. The modification in electronically controlled commutation based on Fourier coefficients for minimizing torque ripple in BLDC motors is presented in [7]. A methodology based on finite-state model predictive control for BLDC motors to reduce commutation torque ripple is proposed in [8]. A vector analysis has been incorporated in a BLDC motor drive and a method of synthesizing the current supply for torque ripple-free operation has been proposed in [9]. Another approach for minimizing commutation torque ripple by implementing a Z-source inverter fed BLDC motor has been explained in [10]. In [11], the technique for torque ripple compensation in a low power BLDC motor is proposed without a DC link capacitor.

In [12,13], the influence of different PWM modes in reducing commutation torque ripple is discussed. The variation in DC input voltage for minimizing torque ripple in a BLDC motor is proposed by Ki-Yong et al. [14]. This method reduces the current ripples and hence torque ripple by varying the input voltage. The current control method using a single DC current sensor is proposed by Joong-Ho [15]. The incoming and outgoing of

*Correspondence: ramyaa@ssn.edu.in

current response are equalized by controlling the duty ratio, thus reducing commutation torque ripple. A new torque control method for minimizing torque ripple is proposed in [16], which generates ideal current pulses with respect to back emf waveforms. Torque ripple minimization by altering the switching angles per half cycle of the inverter is discussed in [17]. The effectiveness of DC voltage control has prompted researchers to analyze several front end converter topologies for torque ripple minimization. In [18,19], the input voltage adjustment for reducing torque ripple is performed by front-end buck and super lift Luo converter. Here the dc link voltage to the inverter is adjusted during conduction and commutation time instants in order to reduce torque ripple. The new circuit topology called a single-ended primary inductor converter (SEPIC) [20] and a modified SEPIC (MSEPIC) converter [21] is employed in front of the inverter to produce the desired dc link voltage to suppress commutation torque ripple. Analysis of the above front-end converter topologies indicates that the response of the converter during commutation instant is vital to minimize torque ripple. In this paper, a front-end circuit topology is proposed with the objective of minimizing commutation torque ripple in a BLDC motor drive. The proposed circuit is composed of an integrated dual output (IDO) converter and a switch selection circuit, which is employed in front of the inverter for the desired DC link voltage selection. The performance of the converter is compared with that of a MSEPIC converter for highlighting the merits of the proposed converter for torque ripple minimization.

2. Modeling and commutation torque ripple analysis of a BLDC motor

The following equations are used to model the BLDC motor [22]. The voltage equation is given as

$$V_{dc} = 2\left[R_s i_a + (L-M)\frac{di_a}{dt}\right] + e_1 - e_2 = R_a i_a + L_a \frac{di_a}{dt} + e_1 - e_2, \tag{1}$$

where L and M are self-inductance and mutual inductance per phase, R_s is the stator winding, e_1 and e_2 are the back EMFs of current carrying phases windings, and i_a is the armature current.

$$R\_a = 2R\_s,\ \Omega \text{ and } L\_a = 2(L-M),\ H \tag{2}$$

The electromagnetic torque developed by the motor can be expressed as T_e,

$$T_e = T_L + J_M \frac{d\omega}{dt} + B_M \omega, \tag{3}$$

where T_L is the load torque, J_M is the inertia, and B_M is the friction constant of the BLDC servomotor. The load torque can be expressed in terms of load inertia J_L and friction B_L components as

$$T_L = J_L \frac{d\omega}{dt} + B_L \omega \tag{4}$$

The output power developed by the motor is

$$P = T_e \omega \tag{5}$$

$$E = e_a = e_b = e_c = K_b \omega, \tag{6}$$

where K_b is back EMF constant, E is back EMF per phase, and ω is the angular velocity in radians per second.

The ideal rectangular current and trapezoidal back emf waveforms of the BLDC motor [23] are shown in Figure 1. However, the influence of resistance and inductance of the motor tends to deviate the current

characteristics at commutation instants where current transitions from one phase to the other phase occur. This deviation of current profile as depicted in Figure 2 is responsible for torque ripple in the BLDC motor drive. Current ripple in the BLDC motor is calculated by the difference in reference and actual current at steady state condition. Torque ripple (TR) is defined as the percentage of difference between the maximum torque (T_{max}) and the minimum torque (T_{min}) to the average torque (T_{avg}) for a particular time interval.

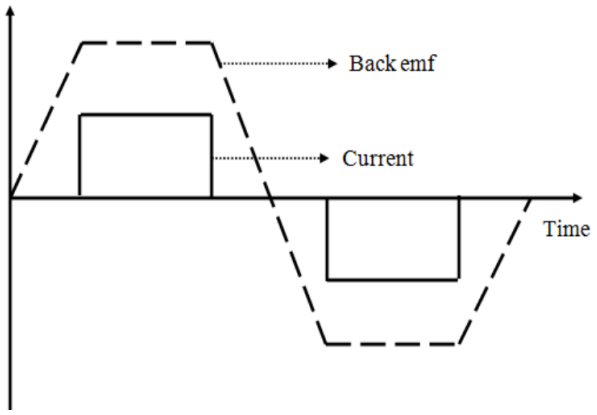

Figure 1. Ideal current and back emf waveform of BLDC motor drive.

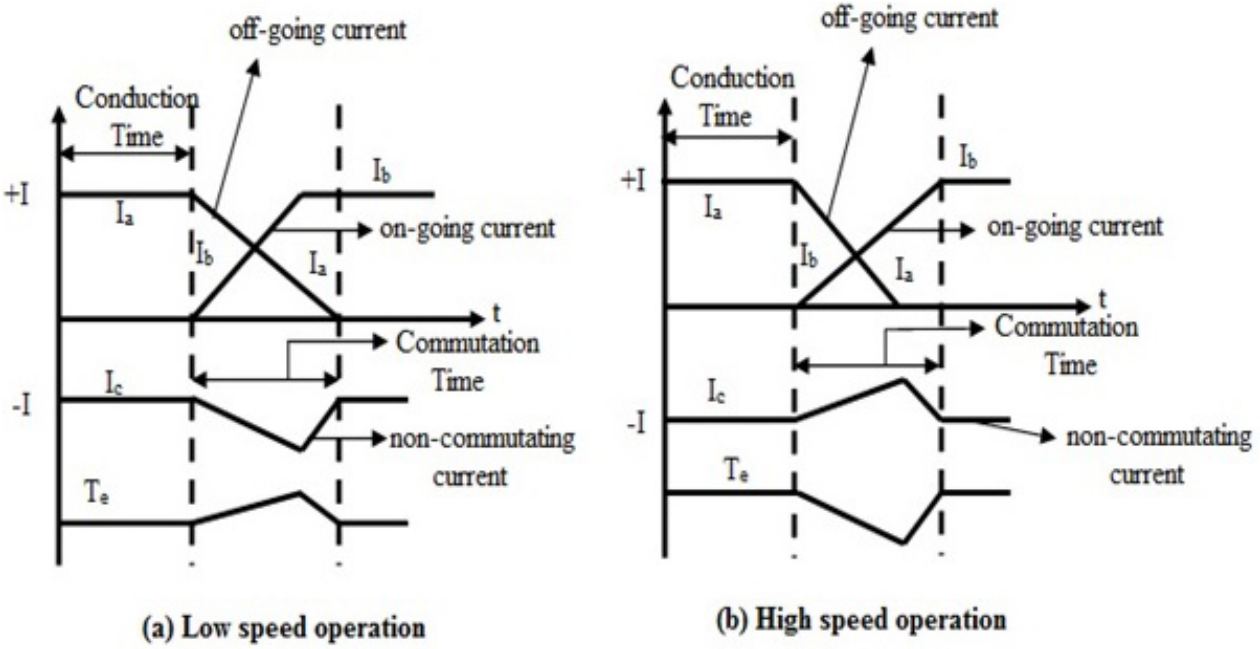

Figure 2. Commutation torque and current of BLDC motor during practical case.

$$TR = \frac{T_{\max} - T_{\min}}{T_{avg}} * 100 \tag{7}$$

To minimize the current deviations and hence torque ripple a front-end integrated dual output (IDO) dc-dc converter is proposed.

3. Integrated dual output dc-dc converter

The circuit topology of the IDO dc-dc converter is shown in Figure 3 and the design parameters are tabulated in Table 1. Here, the two different voltage levels are generated from a single input power source [24]. Here V_{dc} is the input source voltage and V_{01} and V_{02} are the two different levels of output voltage.

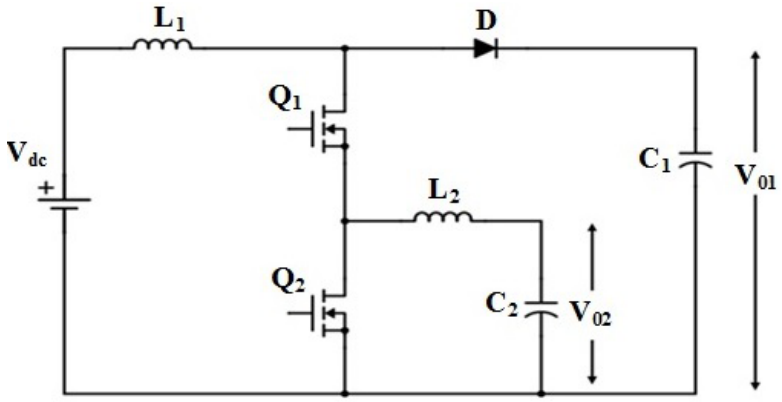

Figure 3. IDO dc-dc converter.

Table 1. Design specifications for IDO converter.

Parameter	Values
Input voltage (V_{dc})	100 V
Step up output voltage (V_{01})	140 V
Step down output voltage (V_{02})	80 V
Switching frequency	50 KHz
Inductor (L_1)	15 μH
Inductor (L_2)	10 μH
Capacitor (C_1)	220 μF
Capacitor (C_2)	550 μF

The IDO converter has two switches Q_1 and Q_2, resulting in three operating states as shown in Figure 4, which are discussed in the following sections.

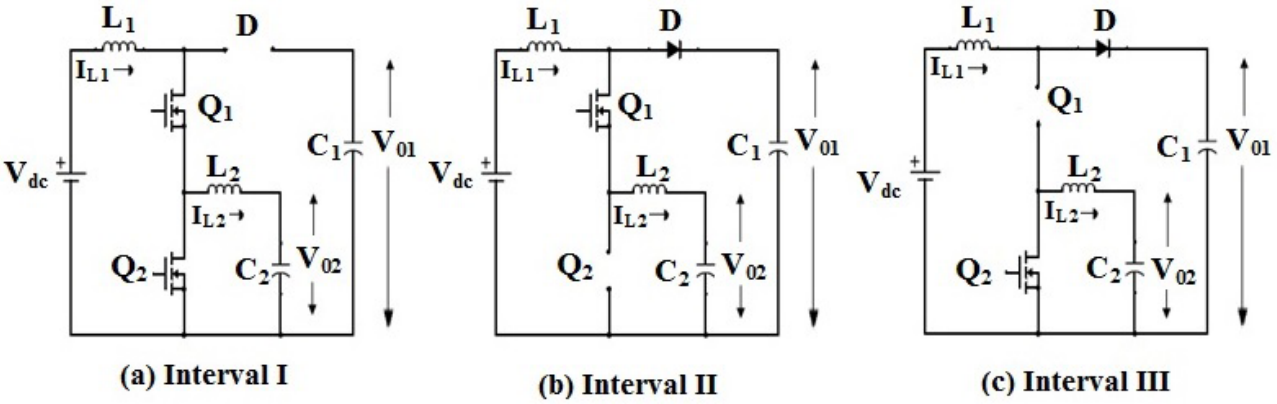

Figure 4. Operating modes of IDO dc-dc converter.

Interval I: In this interval both switches Q_1 and Q_2 are in ON state. Here the diode D_1 is reverse biased and the current I_{L1} passes through the inductor L_1, whereas the inductor current I_{L2} freewheels through the switch Q_2. The duty ratio at this Interval I is defined as D_1.

Interval II: During this interval, switch Q_1 is ON and Q_2 is OFF and the inductor current I_{L1} flows through the diode D_1 and inductor L_2. The diode current is equal to the difference between the inductor currents I_{L1} and I_{L2}. The duty ratio for this interval is defined as D_2.

Interval III: During this interval, the switch Q_1 is OFF and Q_2 is ON. Here the inductor current I_{L2} freewheels through the switch Q_2. Here the two inductors L_1 and L_2 give out the energy to their respective outputs.

The two DC outputs of the IDO converter can be controlled using the corresponding duty cycles D_1 and D_2. The boost mode operates when the switches Q_1 and Q_2 are turned ON simultaneously whereas the buck mode operates when the switch Q_1 is ON and Q_2 is OFF.

The voltage conversion ratio for boost operation is given by

$$\frac{V_{01}}{V_{dc}} = \frac{1}{1 - D_1} \tag{8}$$

Similarly for buck operation is given by

$$\frac{V_{02}}{V_{dc}} = \frac{D_2}{1 - D_1} \tag{9}$$

Thus, the IDO converter has the nature of both boost and buck converters embedded in a single architecture.

4. IDO dc-dc converter fed BLDC motor drive

The block diagram of the BLDC motor drive with the proposed front-end topology is presented in Figure 5. The major challenge in designing a controller for minimizing torque ripple using a front-end converter is to generate the required voltage at conduction and commutation time instants. In the proposed configuration this is achieved with a switch selection circuit that feeds the inverter with the correct voltage level during conduction and commutation time instants by varying the duty cycle of the IDO converter. Throughout the conduction interval the voltage level V_{01} is applied to the inverter circuit in accordance with the speed and load command. During the commutation instant proposed circuit topology regulates the dc link voltage close to $4E_m$ [25] such that the rising and falling speeds of current are equal and hence the torque ripple is reduced. The duty cycle and the regulated dc voltage required under commutation time instants are calculated as follows.

The boost output voltage of the IDO converter, V_{01}, can be calculated as

$$V_{01} = \frac{1}{1 - D_1} * V_{dc}, \tag{10}$$

where D is the duty ratio and V_{dc} is the peak input voltage. The duty ratio for satisfying

V_{01} = 4Em is given by

$$D = \frac{4Ke\omega - Vdc}{4Ke\omega} \tag{11}$$

The flowchart in Figure 6 explains the control algorithm of the BLDC drive for torque ripple minimization with the proposed front-end converter.

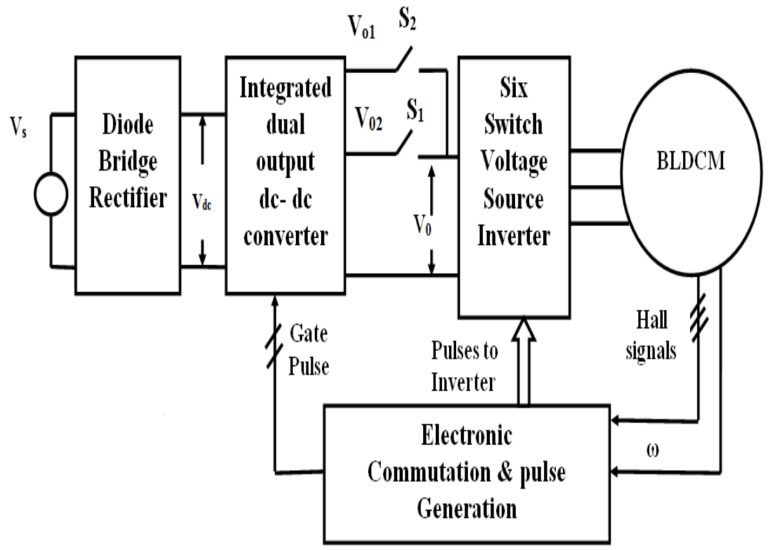

Figure 5. Block diagram of BLDC motor drive with proposed control strategy.

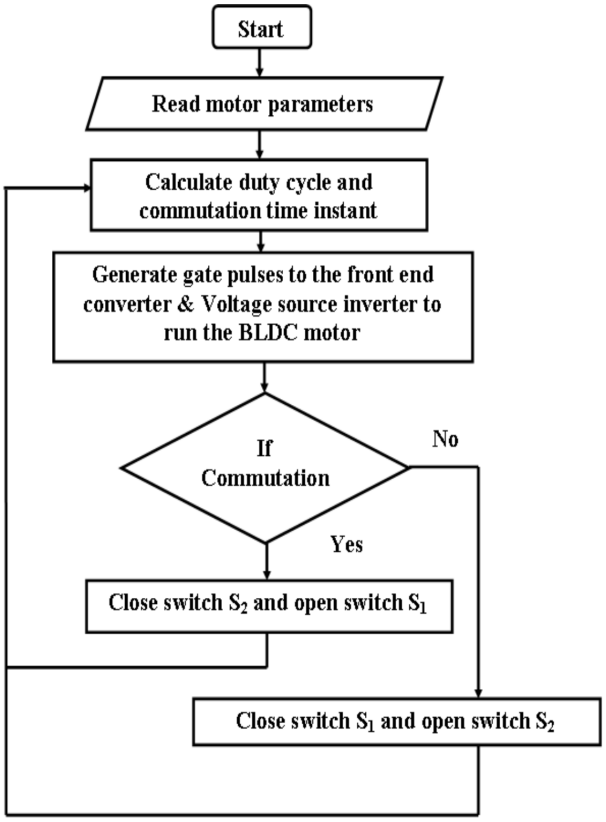

Figure 6. Flowchart of the control algorithm.

5. Results and discussion

To analyze the performance of the BLDC motor drive with an IDO converter the simulation is done in MATLAB/Simulink environment. The parameters of the surface mounted BLDC motor used in this work are tabulated in Table 2.

Table 2. BLDC motor parameters.

Voltage	310 V
Rated current	4.52 A
Rated speed	4600 rpm
Rated power	1 hp
Stator phase resistance	3.07 Ω
Stator phase inductance	6.57 mH
Inertia	1.8e^{-4} kg-m^2

The conventional BLDC drive schematic without dc link voltage control is shown in Figure 7 and the torque ripple for the conventional method is indicated in Table 3 for different speeds. The robustness of the controller with the IDO converter fed BLDC motor is illustrated through the current, torque, and speed response with load and speed variation as shown in Figures 8 and 9, respectively.

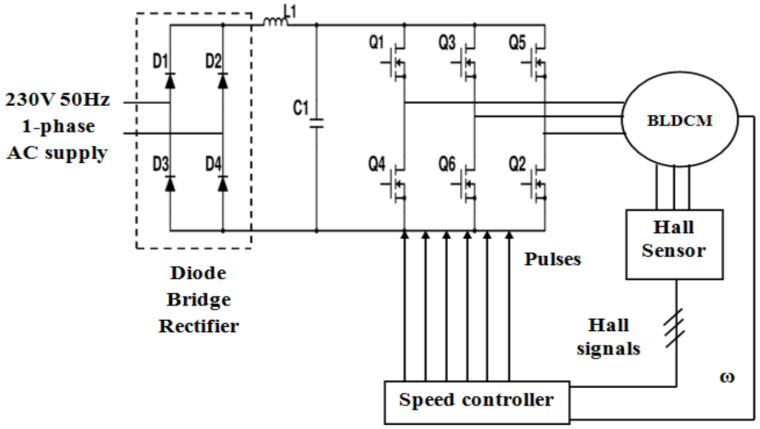

Figure 7. Schematic block diagram of the conventional BLDC motor drive.

Table 3. Torque ripple in conventional BLDC motor drive.

Speed (rpm)	% Torque ripple
100	14.69
300	29.67
1000	44.87

To highlight the effectiveness of the proposed front-end IDO based DC-DC converter topology, simulation of the BLDC drive as shown in Figure 5 is performed to evaluate torque ripple under various loading conditions. The phase currents of the BLDC motor drive with and without and the IDO converter at 1000 rpm speed and 0.5 Nm load with same operating conditions are compared in Figure 10. From the waveforms it is observed that the spikes during commutation time instant are smooth and the current is much closer to the ideal current waveform in the proposed topology. Figure 11 shows the electromagnetic torque response with and without the proposed topology. From the waveforms it is observed that the torque pulsations at commutation time instants are reduced in the proposed topology. The variation in DC link voltage at commutation instant of the IDO converter for different speeds is shown in Figure 12.

The efficacy of the proposed control strategy is demonstrated by comparing the results of a conventional control scheme and a MSEPIC-based BLDC motor drive with the proposed configuration and the values of

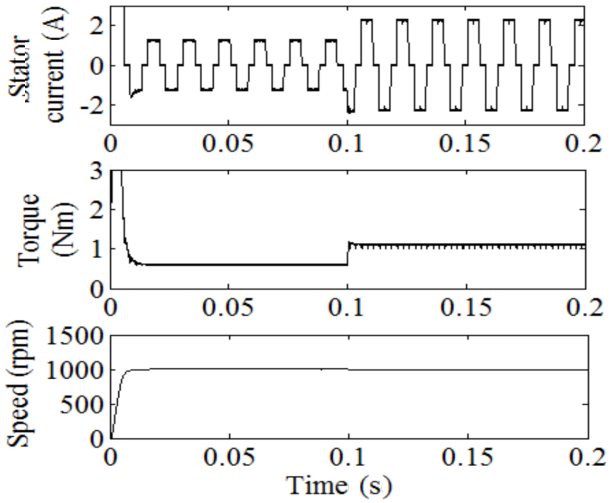

Figure 8. Simulated current, torque, and speed response for the proposed IDO converter based BLDC drive system with load variation.

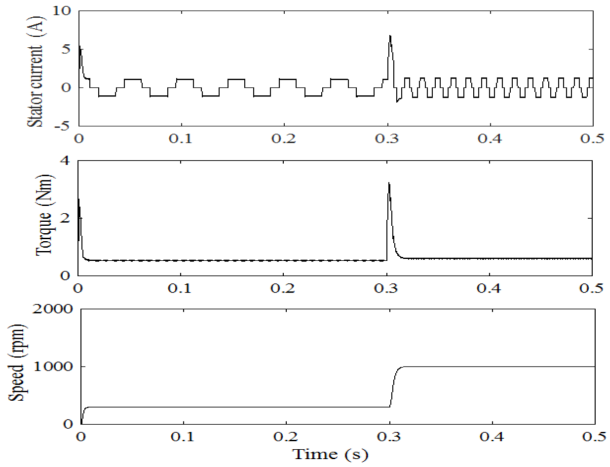

Figure 9. Simulated current, torque, and speed response for the proposed IDO converter based BLDC drive system with speed variation.

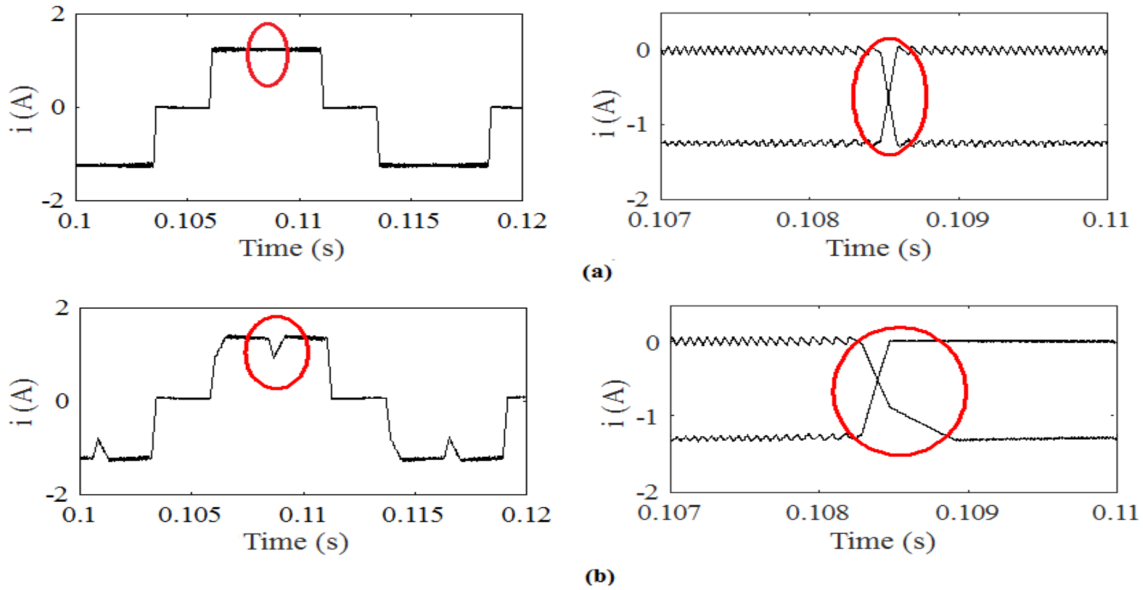

Figure 10. Phase currents at 1000 rpm. (a) With dc link voltage control by an IDO converter. (b) Without dc link voltage control.

torque ripples for various speeds are shown in a chart in Figure 13. Similarly, the torque ripple reduction ratio of the proposed topology with the conventional method and MSEPIC topology is tabulated in Table 4. The results reveal that the torque ripple in the IDO-based drive is less when compared to the conventional and MSEPIC-fed BLDC motor drive.

The simulation results are validated with the experimental setup as shown in Figure 14. The inverter module comprises IGBT switches rated at 600 V and 10 A with a switching frequency of 10 kHz. A Xilinx SPARTAN 3E FPGA kit with 25 MHz frequency is used to provide gating signals to inverter switches in accordance with the three Hall position sensor signals and reference speed information. The PWM pulses to

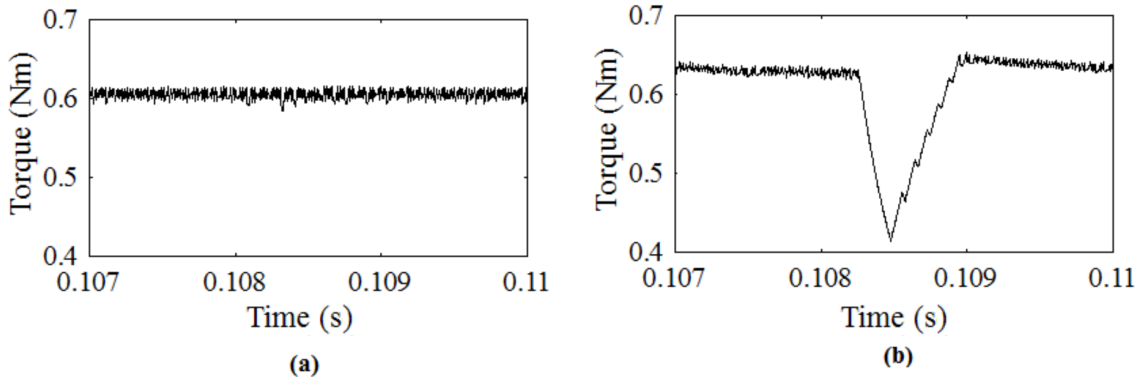

Figure 11. Electromagnetic at 1000 rpm. (a) With dc link voltage control by an IDO converter. (b) Without dc link voltage control.

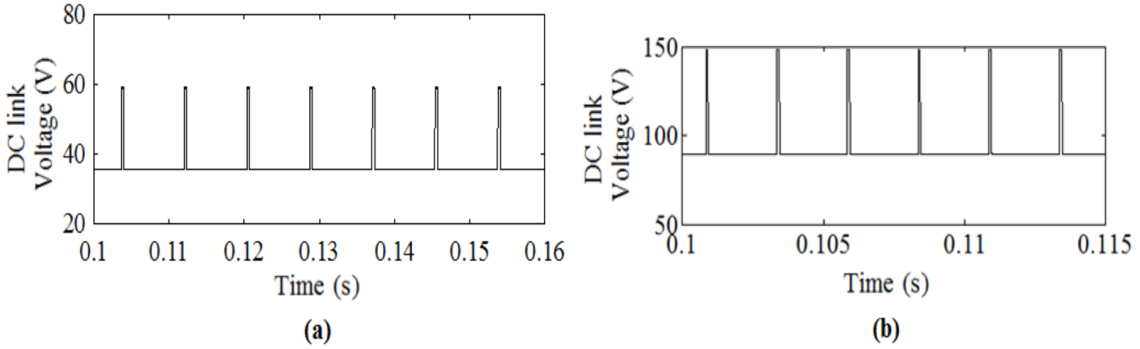

Figure 12. Dc link voltage at (a) 300 rpm, (b) 1000 rpm.

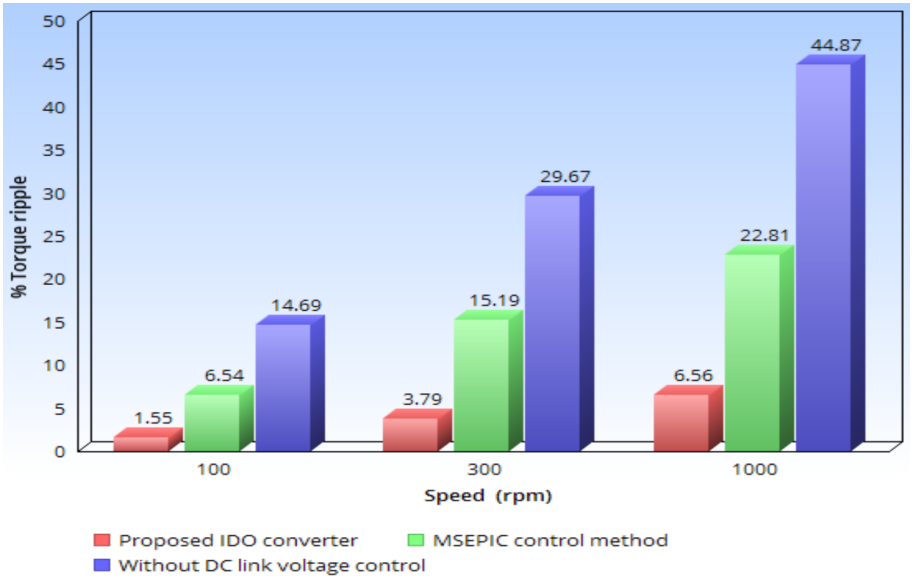

Figure 13. Comparison of torque ripple of proposed IDO converter with conventional and MSEPIC control.

the inverter are obtained from 6 I/O lines of the Xilinx-FPGA SPARTAN 3E board. The control algorithm is implemented in the Xilinx FPGA kit using a MATLAB system generator.

Table 4. Torque ripple reduction ratio of proposed topology with conventional and MSEPIC topology.

Speed (rpm)	% Reduction of torque ripple in proposed IDO converter	
	With conventional method	With MSEPIC control method
100	13.1%	4.99%
300	25.8%	11.4%
1000	38.3%	16.2%

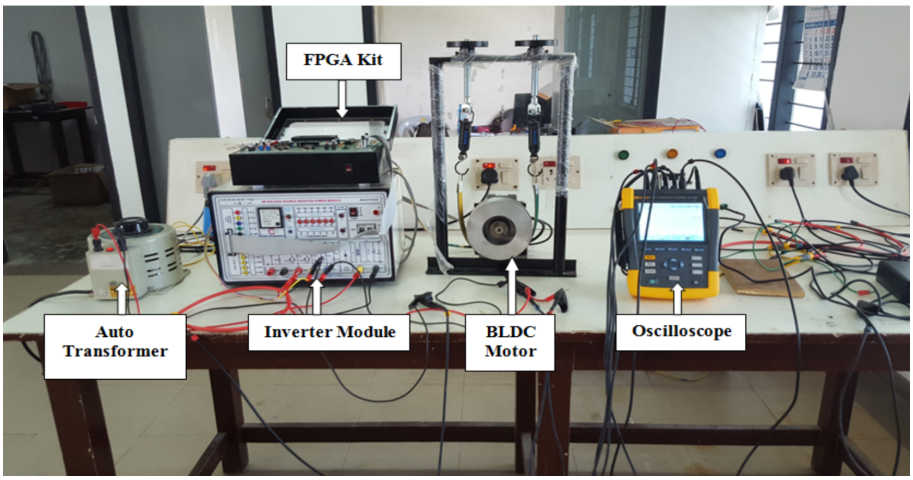

Figure 14. Experimental setup of the BLDC motor drive.

Figure 15 shows the experimental and simulated speed response for the closed loop operation of the BLDC motor. Figures 16 and 17 show the experimental phase current waveforms at 300 rpm and 1000 rpm. The simulation and the experimental results disclose a close correlation, which indicates the suitability of the proposed method for torque ripple minimization.

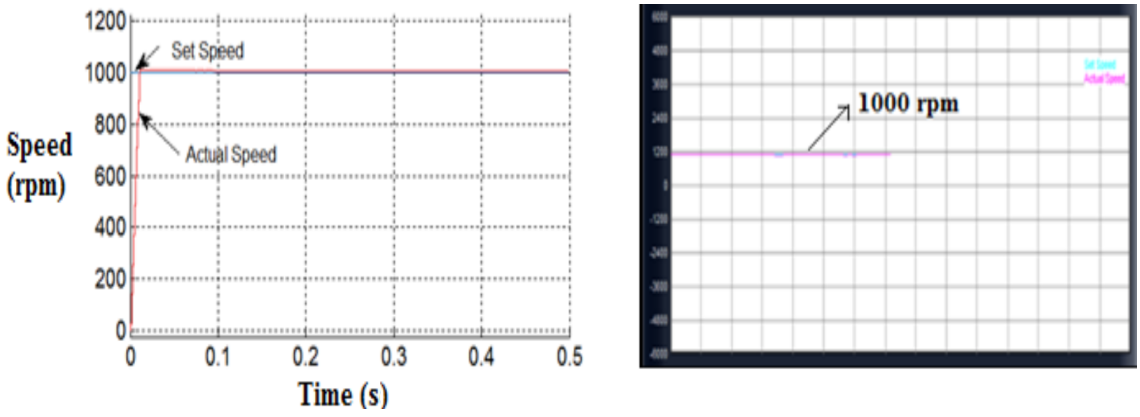

Figure 15. Experimental and simulated speed response.

6. Conclusion

In this paper, integrated dual output-based front end dc-dc converter topology for torque ripple minimization is proposed. The voltage levels of the proposed topology are varied during conduction and commutation instants

according to the speed and load variations. From the results it is observed that a considerable reduction in torque ripple is achieved in comparison with the conventional BLDC drive and MSEPIC converter fed drive. Hardware validation of the conventional drive is done to substantiate the simulation results. The fast voltage adjustment feature of the topology with minimum components augurs well for its suitability in variable speed applications.

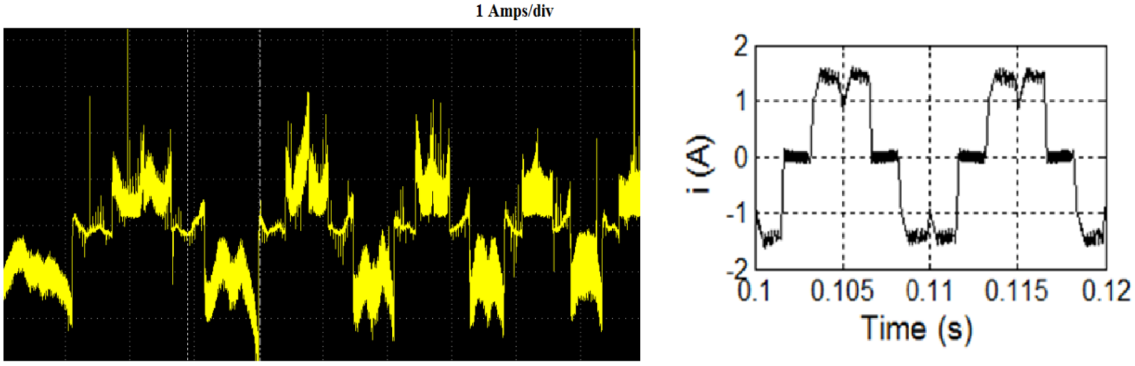

Figure 16. Experimental and simulated current response for 300 rpm.

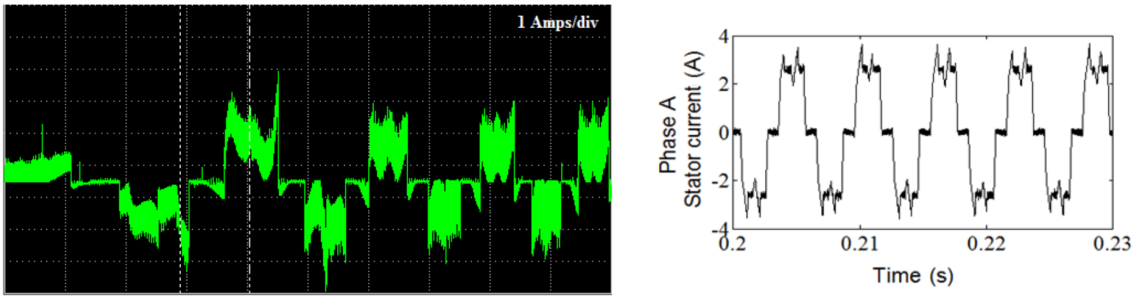

Figure 17. Experimental and simulated current response for 1000 rpm.

References

[1] Rodriguez F, Emadi A. A novel digital control technique for brushless DC motor drives. IEEE T Ind Electron 2007; 54: 2365-2373.

[2] Sathyan A, Milivojevic N, Lee YJ, Krishnamurthy M, Emadi A. An FPGA-based novel digital PWM control scheme for BLDC motor drives. IEEE T Ind Electron 2009; 56: 3040-3049.

[3] Milivojevic N, Krishnamurthy M, Gurkaynak Y, Sathyan A, Lee YJ, Emadi A. Stability analysis of FPGA-based control of brushless DC motors and generators using digital PWM technique. IEEE T Ind Electron 2012; 59: 343-351.

[4] Aydogdu O, Akkaya R. An effective real coded GA based fuzzy controller for speed control of a BLDC motor without speed sensor. Turk J Elec Eng & Comp Sci 2011; 19: 413-430.

[5] Yadav P, Poova R, Najamudeen K. High dynamic performance of a BLDC motor with a front end converter using an FPGA based controller for electric vehicle application. Turk J Elec Eng & Comp Sci 2016; 24: 1636-1651.

[6] Zerollg H, Boukais B, Sahraui H. Analysis of torque ripple in a BDCM. IEEE T Magn 2002; 38: 1293-1296.

[7] Aghili F. Ripple suppression of BLDC motors with finite driver/amplifier bandwidth at high velocity. IEEE T Contr Syst T 2011; 19: 391-397.

[8] Xia C, Wang Y, Shi T. Implementation of finite-state model predictive control for commutation torque ripple minimisation of permanent magnet brushless DC motor. IEEE T Ind Electron 2013; 60: 896-905.

[9] Buja G, Bertoluzzo M, Keshri RK. Torque ripple free operation of PMBLDC drives with petal wave current supply. IEEE T Ind Electron 2015; 62: 4034-4043.

[10] Li C, Xia C, Cao Y, Chen W, Shi T. Commutation torque ripple reduction strategy of Z-source inverter fed brushless DC motor. IEEE T Power Electr 2016; 31: 7677-7690.

[11] Ransara HKS, Madawala UK. A torque ripple compensation technique for a low cost brushless DC motor drive. IEEE T Ind Electron 2015; 62: 6171-6182.

[12] Carlson R, Mazenc ML, Fagundes JC. Analysis of torque ripple due to phase commutation in brushless dc machines. IEEE T Ind Appl 1992; 28: 632-638.

[13] Xiandun Z, Boshi C. Influences of PWM mode on the current generated by BEMF of switch-off phase in control system of BLDC motor. In: IEEE 2001 Electrical machines and systems Conference; 18–20 August 2001; China. pp. 579-582.

[14] Nam KY, Lee WT, Lee CM, Hong JP. Reducing torque ripple of brushless DC motor by varying input voltage. IEEE T Magn 2006; 42: 1307-1310.

[15] Song JH, Choy I. Commutation torque ripple reduction in brushless DC motor drives using a single DC current sensor. IEEE T Power Electr 2004; 19: 312-319.

[16] Lu H, Zhang L, Qu W. A new torque control method for torque ripple minimization of BLDC motors with un-ideal back EMF. IEEE T Power Electr 2008; 23: 950-958.

[17] Kim YH, Cho BG, KO Y. Generalized techniques of reducing torque ripples in BDCM drives. In: IEEE 1994 Industrial Electronics Control and Instrumentation Conference; 5–9 September 1994; Bologna, Italy. pp 514-519.

[18] Zhang XF, Lu ZY. A new BLDC motor drives method based on BUCK converter for torque ripple reduction. In: IEEE 2006 Power Electronics and Motion Control Conference; 14–16 August 2006; Shanghai, China. pp. 1-4.

[19] Chen W, Xia CL, Xue M. A torque ripple suppression circuit for brushless DC motors based on power dc/dc converters. In: IEEE 2008 Industrial Electronics and Application Conference; 3–5 June 2008; Singapore. pp. 1453-1457.

[20] Shi T, Guo Y, Song P, Xia C. A new approach of minimizing commutation torque ripple for brushless DC motor based on DC–DC converter. IEEE T Ind Electron 2010; 57: 3483-3490.

[21] Ramya A, Srinath V, Samyuktha S, Vimal R, Balaji M, Commutation torque ripple reduction in brushless DC motor using modified SEPIC converter. In: IEEE 2015 Power Electronics Drives and Systems; 9–12 June 2015; Sydney, Australia. pp. 307-312.

[22] Bayoumi EHE, Soliman HM, Awadallah MA. Adaptive deadbeat controllers for brushless Dc drives using PSO and ANFIS techniques. J Electr Eng 2009; 60: 3-11.

[23] Liu Y, Zhu ZQ, Howe D. Commutation-torque-ripple minimization in direct-torque-controlled PM brushless DC drives. IEEE T Ind Appl 2007; 43: 1012-1021.

[24] Ray O, Josyula AP, Mishra S, Joshi A. Integrated dual-output converter. IEEE T Ind Electron 2015; 62: 371-382.

[25] Ashabani M, Kaviani AK, Milimonfared J, Abdi B. Minimization of commutation torque ripple in brushless dc motors with optimised input voltage control. In: IEEE 2008 Power Electronics, Electrical Drives, Automation and Motion Symposium; 11–13 June 2008; Italy. pp 250-255.